Towing Tank and Flume Testing of Passively Adaptive Composite Tidal Turbine Blades

Robynne E. Murray*, Stephanie Ordonez-Sanchez†, Kate E. Porter†, Darrel A. Doman‡, Michael J. Pegg§, and Cameron M. Johnstone†

*robynne.murray@nrel.gov, National Renewable Energy Laboratory, 15013 Denver West Parkway, Golden, CO, USA 80401

†Department of Mechanical and Aerospace Engineering, University of Strathclyde, Glasgow, UK G1 1XJ

‡Department of Mechanical Engineering, Dalhousie University, Halifax, Nova Scotia, Canada B3H 4R2

§Department of Process Engineering and Applied Science, Dalhousie University, Halifax, Nova Scotia, Canada B3H 4R2

***Abstract*—**Composite tidal turbine blades with bend-twist (BT) coupled layups allow the blade to self-adapt to local site conditions by passively twisting. Passive feathering has the potential to increase annual energy production and shed thrust loads and power under extreme tidal flows. Decreased hydrodynamic thrust and power during extreme conditions means that the turbine support structure, generator, and other components can be sized more appropriately, resulting in a higher utilization factor and increased cost effectiveness.

This paper presents new experimental data for a small-scale turbine with BT composite blades. The research team tested the turbine in the Kelvin Hydrodynamics Laboratory towing tank at the University of Strathclyde in Glasgow, United Kingdom, and in the recirculating current flume at the l'Institut Français de Recherche pour l'Exploitation de la Mer Centre in Boulogne-sur-Mer, France. Tests were also performed on rigid aluminum blades with identical geometry, which yielded baseline test sets for comparison. The results from both facilities agreed closely, supporting the hypothesis that increased blade flexibility can induce load reductions. Under the most extreme conditions tested the turbine with BT blades had up to 11% lower peak thrust loads and a 15% reduction in peak power compared to the turbine with rigid blades. The load reductions varied as a function of turbine rotational velocity and ambient flow velocity.

***Keywords*—composite materials, bend-twist coupling, towing tank testing, flume testing, load reductions**

I. Introduction

The cost to deploy horizontal-axis tidal turbines (HATTs) and access them for maintenance in harsh offshore environments makes up a large percentage of the required investment for a commercial tidal turbine. Using current estimates, manufacturing and deploying a tidal turbine account for 53.3% of the cost of energy, and operating and maintaining a HATT make up 30% of its total levelized cost of energy [1]. This means that reliability and survivability, as well as turbine component weight, are key areas of development in the tidal energy industry [2,3]. In addition, blade weight and rotor loads contribute significantly to the physical demands on the hub and support structure, affecting the size requirements of turbine components (e.g., hub, bearings, and drivetrain, among others). This has implications on transporting, deploying, and retrieving the turbine, as well as on the capital requirements for the support structure. All these factors make up a significant percentage of the turbine capital cost [4]. To reduce component weight and increase strength and durability, turbine blades are typically manufactured from fiber-reinforced composite materials.

Composite materials are advantageous due to their higher strength-to-weight ratios, increased corrosion resistance, high fatigue tolerance, and higher damage tolerance than most metal materials [5,6]. Composite materials can also be specifically tailored to manipulate the mechanical response of the blade [7]. By preferentially orienting the fibers at an angle to the long axis of the blade, the flap-wise bending can be coupled with span-wise twisting (bend-twist [BT] coupling). BT coupling alters the angle of attack of the blade as a function of the hydrodynamic loading. If the blade's fibers are oriented appropriately, it can passively feather, reducing blade and structural loads. Reduced loads on the blades lead to decreased loads on other turbine components, including the turbine support structure, allowing smaller and less expensive components to be used.

BT-coupled composite blades also have the potential to regulate turbine power production at off-design conditions. This reduces the demands on the turbine generator and increases the utilization factor of the turbine. Other potential benefits of such blades are increased efficiency and annual energy production; increased hydrodynamic stability; delayed cavitation inception [8]; and a reduced risk of mechanical failure, which leads to costly maintenance, particularly for fixed-pitch blades. BT coupling has also been used in the propulsion and wind energy industries, with the benefits of these applications outlined in previous work [9].

A. Objectives

Research in the tidal energy industry has demonstrated the potential for load reductions and power regulation through numerical modeling of turbines with BT composite blades [7,8,10]. However, experimental data for verification of turbine models with flexible blades are lacking, necessitating high safety factors in turbine and blade design to compensate for the uncertainty in turbine loads.

The objective of this work is to quantify the performance of an 828-mm-diameter, three-bladed HATT with BT composite blades. The HATT was tested in the Kelvin Hydrodynamics Laboratory towing tank at the University of Strathclyde, Glasgow, United Kingdom, and in the recirculating current flume at the l'Institut Français de Recherche pour l'Exploitation de la Mer (IFREMER) Centre in Boulogne-sur-Mer, France. Throughout this test program, the turbine was operated with geometrically equivalent rigid aluminum blades, facilitating a comparison between BT composite and rigid blades. The two test facilities also differed in operation and turbulence levels, enabling a comparison of turbine performance in different test conditions. This is an important consideration when comparing results of scale model tests and making full scale turbine performance predictions. These tests are intended to increase confidence in turbine performance modeling by yielding model verification data for a range of operating conditions.

II. Experimental Setup

Small-scale turbines are often used for proof-of-concept testing and numerical model verification (work performed at technology readiness levels of 3–4 [11]) because they are more cost-effective than full-scale testing [12]. In this work, an 828-mm-diameter turbine was chosen to compromise between maximizing the Reynolds number and minimizing the blockage ratio, which was 4.6% in the towing tank and 6.7% in the flume. The team did not consider these values large enough to require correction [13]. This section details the test program and conditions, the experimental setup, and the blade and turbine geometry.

A. Test procedure

Table 1 summarizes the facilities and test conditions.

Table 1 Summary of test facilities and conditions.

	Kelvin Hydrodynamics Laboratory	IFREMER Centre
Facility dimensions	76 m × 4.6 m × 2.5 m	18 m × 4 m × 2 m
Flow velocities tested	0.85 m/s and 1.0 m/s	0.80 m/s, 1.0 m/s and 1.2 m/s
Turbulence intensity	0%	1.46%
Blockage ratio	4.6%	6.7%

The desired outcome of this test program was a set of performance curves for a turbine with both composite BT and aluminum blades from different test facilities. To achieve this, primarily flow speeds of 1.0 m/s were tested (carriage speed in the towing tank and current speed in the flume are both referred to as flow speeds). However, tests were also performed at 0.80 m/s and 1.2 m/s in the flume, and at 0.85 m/s in the towing tank. At both facilities the rotor rotational speeds were varied between 50 and 110 rpm in increments of 5 rpm. For each test the rotational velocity and flow velocities were fixed, producing data for a single tip-speed ratio (λ). These test conditions resulted in chord-Reynolds numbers ranging from 8×10^4 to 1.7×10^5 based on a chord length of 0.047 m at 75% radius.

The flow velocity, rotor torque, thrust, and rotational speeds were averaged over the steady region of each test. Based on the carriage speeds and towing tank length, this resulted in a test length of approximately 30 s for the towing tank tests. Flume tests were run for 300 s each. Noise in the raw thrust and torque signals was Gaussian with a zero mean. Calibration factors were determined prior to testing and applied to the raw data to convert that data to engineering units. To represent the turbine loads and power in nondimensional terms commonly used in the industry, thrust and power coefficients were calculated as outlined in [14].

B. Experimental setup and instrumentation

Figure 1 shows the test turbine, which was designed and manufactured at Cardiff University (Cardiff, Wales) [15]. The same test equipment was used in both the towing tank and flume facilities, with the exception of the data acquisition. The turbine was rotated at a constant rotational speed using a Rexroth IndraDyn Synchronous-Torquemotors motor. To obtain the rotor torque produced by the blades, the motor torque generating current (TGC) required to rotate the turbine at a particular speed without the blades was subtracted from the TGC recorded for each test (with the blades on). The TGC, which is a function of the rotational speed of the motor, was calibrated by the Cardiff team before testing. More details on the TGC and rotor torque calculations can be found in [16].

To measure the thrust on the rotor, a 5-mm-long, Y11-FA-5-120 strain gauge was instrumented in a full bridge configuration on the turbine stanchion 1.5 m from the midhub height (0.5 m above the free surface). This was calibrated by applying loads to a lever arm and measuring the output voltage, which produced a linear relationship with high coefficient of determination. To isolate the thrust loads on the blades, tests were also run without the blades at a range of flow speeds. This enabled the thrust associated with the support structure at the appropriate flow velocity to be subtracted from the mean thrust measured for each test.

Kelvin Hydrodynamics Laboratory, United Kingdom

The turbine was secured to the towing tank in the Kelvin Hydrodynamics Laboratory via a vertical stanchion mounted to the carriage structure by two brackets. The center of the hub was positioned 1.0 m below the free surface of the water. Figure 1 shows the turbine—fitted with the composite BT blades—installed in the towing tank.

Data from the towing tank tests was logged at 137 Hz using the Cambridge Electronic Design Power 1401 DAQ and the DAQ program, Spike, and exported as text files for post processing in MATLAB. A position output from the motor drive was used in conjunction with a time stamp recorded in Spike to obtain the rotational speed of the rotor. The carriage speed was specified and tracked using the carriage control

system. For comparison to the flume tests, the turbulence intensity in this case can be assumed to be zero because the tank was given time to settle between tests.

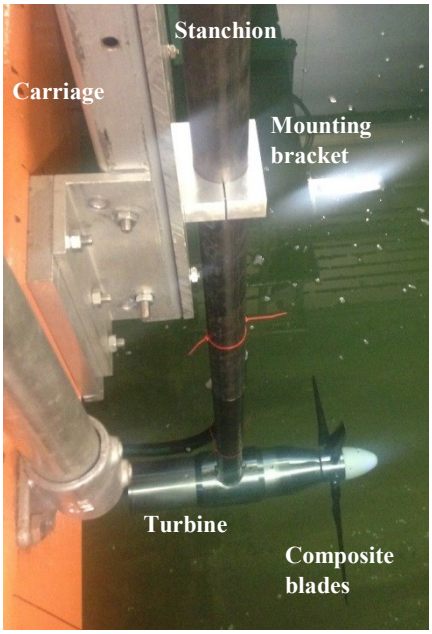

Figure 1 Cardiff University turbine fitted with the composite BT blades and installed in the towing tank at the Kelvin Hydrodynamics Laboratory.

IFREMER Centre, France

Figure 2 shows the turbine mounted in the flume at IFREMER. The stanchion was fixed with two brackets to a steel construction support frame mounted on a crossbeam over the flume. The middle of the hub was 1.0 m below the free surface of the water.

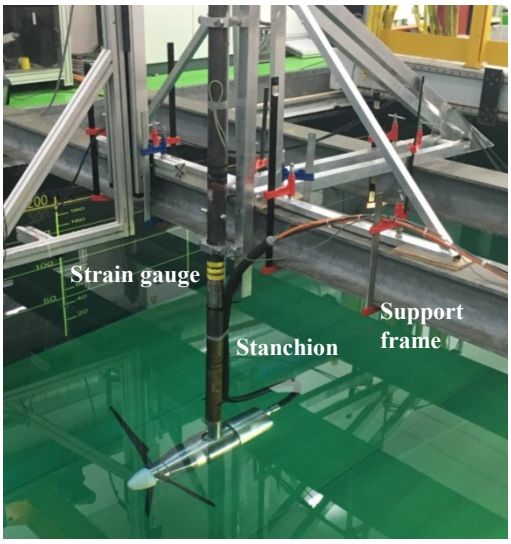

Figure 2 Cardiff University turbine fitted with the composite BT blades and installed at the IFREMER Centre.

For the flume tests, the flow velocity was monitored during testing using a laser Doppler velocimeter that recorded the flow velocities in the x and y directions at a minimum resolution of 56 Hz at the midhub height (a distance of 3.6 m upstream of the turbine). The average turbulence intensity for a point at the midhub level was 1.46%.

For the flume tests, data were logged using a National Instruments LabVIEW data acquisition system at a sampling frequency of 250 Hz. The rotational speed was a direct output of the motor control system into LabVIEW.

C. Rotor geometry

The rotor had a radius of 414 mm, with a hub radius of 50 mm, a blade length of 364 mm, and a blade root pitch setting of 28.89º ± 0.38º (relative to the rotor plane). This pitch setting was fixed using a grub screw that fitted into a slot on the blade root. A 40-mm-long root section was tapered from a 29-mm-diameter circular cross section to the first National Renewable Energy Laboratory (NREL) S814 airfoil shape at 68 mm from the base of the blade. The NREL S814 airfoil shape was used for a 292-mm-long working section. Details of the blade geometry, including the chord length and pretwist, are given in [13].

D. Blade design and materials

The composite blades, shown in Figure 3, were manufactured by Airborne Marine, Netherlands. A fluid-structure interaction (FSI) design tool described in [10] was used to guide the design (ply angles, ply thicknesses, and materials) of the BT composite blades. The objective of the design process was to maximize the induced twist response of the blade while keeping the composite stresses to an allowable limit.

To meet strength requirements but maintain sufficient flexibility for passive twisting, the blades were constructed with a Sicomin PB 250 [17] epoxy-closed-cell foam core with composite overlay skins. The working section of the blade had a single layer of 0.20-mm-thick unidirectional graphite epoxy composite with fibers oriented at an angle of 26.8° from the long axis of the blade. The upper and lower composite skins had a mirror layup, as detailed in [18], to induce BT coupling. Figure 3 shows the composite blades during and after manufacturing, along with the aluminum blades.

Figure 3 Photographs of blades: (left) composite blades during manufacturing [19]; (middle) composite blades; and (right) aluminum blades.

A 40-mm-long, 25.4-mm-diameter cylindrical steel insert was used for strength at the blade root, as shown in Figure 3. The root section (from the circular insert to the first NREL S814 airfoil cross section) had six additional 0.2-mm-thick composite layers at alternating ply angles of [15º,–15º].

The steel insert and the composite skins are visible inside the blade mold in Figure 3. A 15-mm-diameter steel extension protruded from the 25.4-mm steel root to connect the blades to the test turbine (as shown in the image of the aluminum blades in Figure 3). Table 2 gives material properties.

Table 2 Composite and epoxy material properties [17, 20]

Graphite-Epoxy Properties		Sicomin Epoxy Properties	
Young's modulus, longitudinal	126 GPa	Density	250 kg/m^3
Young's modulus, transverse	7.7 GPa	Compressive modulus	0.0189 GPa
Shear modulus	3.9 GPa	Shear modulus	0.0073 GPa
Poisson's ratio	0.335	Poisson's ratio	0.3

As a reference against which to quantify the BT blade performance, aluminum blades were manufactured using a 5-axis CNC machine from a CAD model based on a 3-D scan of the composite blades. After manufacturing, epoxy was applied to fill any small grooves and 400/P800 grit abrasive paper was used to smooth the surface of the blades, making the final surface finish similar to that of the composite blades.

E. Structural comparison

The towing tank tests were designed to compare the hydrodynamic response of a turbine with BT composite blades to that of one with rigid blades. To verify that the aluminum blades were effectively rigid compared to the BT blades, structural bending tests were undertaken for both sets of blades. The blades were constrained at the root, and a point load was applied along the span. The displacement was measured using an optical tracking system with the LabVIEW Vision Development module. More detail on these tests can be found in [10].

Figure 4 shows the bending displacement of all three composite BT blades compared to one of the aluminum blades. The bending displacement of both blade sets was linear for this range of applied loads. For a maximum applied tip load of 45 N, the bending displacement of the aluminum blades was less than 1.5 mm. For an applied load of 25 N, the aluminum blade had 84% less bending displacement compared to the composite blades.

Although not shown here, the twist of the aluminum blade was less than 1% of that measured for the composite BT blades. For the purposes of this work, the aluminum blades were considered rigid relative to the composite BT blades. From Figure 4, one of the composite blades had slightly more bending deformation than the other two. Based on optical measurements of the longitudinal fiber direction relative to the blade's long axis, the ply angles for composite blade 1.3 were about 2° greater than the other two blades, resulting in less resistance to bending.

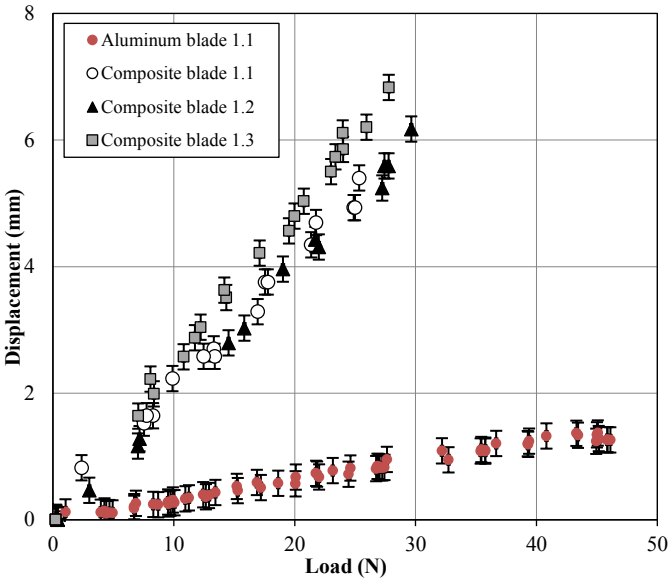

Figure 4 Load versus bending displacement for aluminum and composite blades.

III. Results and Discussion

This section presents the thrust and power results for the turbine with BT composite blades compared to rigid aluminum blades at both test facilities. A spectral analysis of the thrust signal is also presented in this section.

A. Uncertainty analysis

The error bars shown on the data presented in this section were calculated based on the uncertainty analysis methods presented in EquiMar deliverable 3.4 [21] and the International Towing Tank Conference protocol [22]. To estimate the precision error of the tests, five tests were repeated under the same conditions at both facilities.

For the towing tank tests, the combined expanded uncertainty for the thrust measurement was found to be less than 2% for all tests. This resulted from the high repeatability of the thrust measurements and the high coefficient of determination obtained during the strain gauge calibration. Greater scatter in the torque measurements for the repeat tests, however, resulted in a combined expanded uncertainty as a percentage of the mean torque, which increased to more than 6% for λ greater than 4.5. The uncertainty in the λ, based on the uncertainty in the flow speed, rotational speed, and turbine radius, was less than 1% for all tests.

For the flume tests, the combined expanded uncertainty was found to be less than 5% for the thrust measurements and less than 7% for the torque measurements. The uncertainty in the λ measurement was less than 2% for all tests. The slightly higher uncertainty in the flume tests resulted from greater uncertainty in the motor calibration for this set of tests, as well as from different processing equipment for the strain gauges.

B. Rotor thrust loads

Figure 5 shows the rotor thrust as a function of rotational speed (rpm) for a turbine with composite BT and aluminum blades at 1.0 m/s. Figure 6 shows the thrust loads for both the composite and aluminum blades for the various flow speeds

tested at both facilities. Error bars are shown in Figure 5, but were omitted from Figure 6 for clarity. Details of the experimental uncertainty are given in Section III-C.

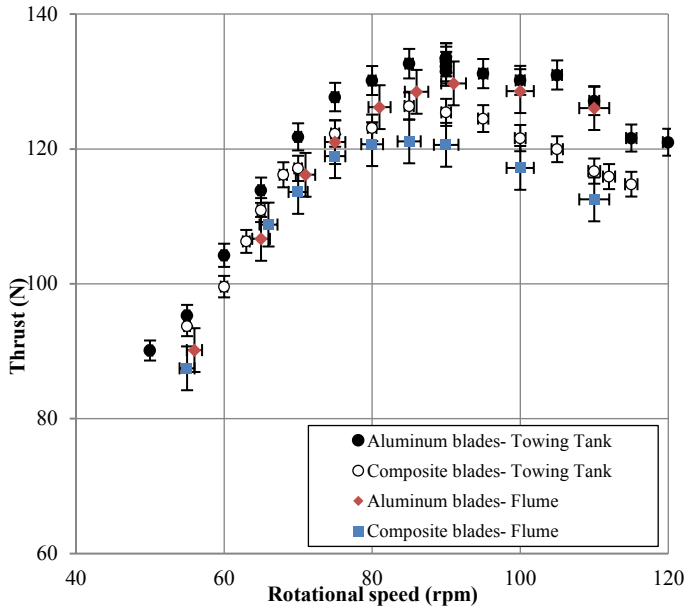

Figure 5 Rotor thrust for composite BT blades and rigid aluminum blades. Flow speed was1.0 m/s and rotational speeds varied.

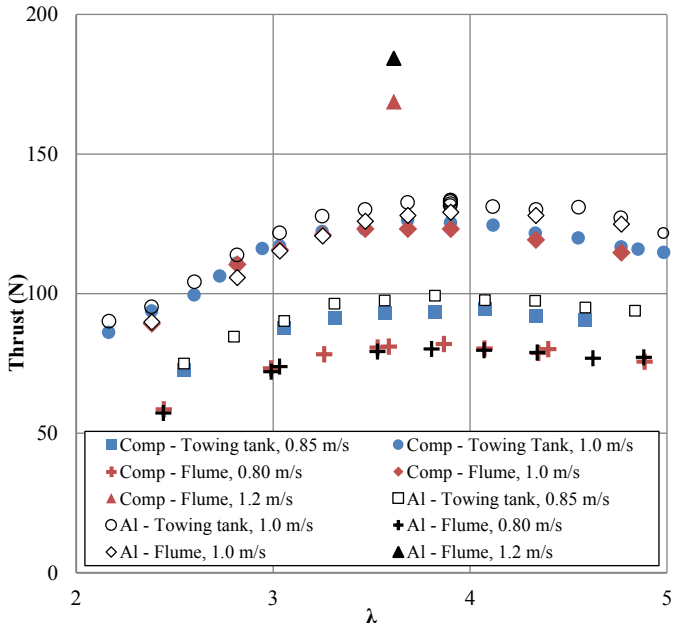

Figure 6 Rotor thrust for composite BT blades and rigid aluminum blades. Flow and rotational speeds varied.

From Figure 5, the difference in thrust loads between the blade types increased with the rotor rotational speed. The turbine with BT composite blades had up to 7% lower thrust loads measured in the towing tank and 9% lower thrust loads in the flume, at 1.0 m/s. BT blade thrust load reductions also increased with increasing flow speeds. This is apparent in Figure 6, which illustrates an 11% reduction in thrust loads for the BT blades at a flow speed of 1.2 m/s compared to the lower flow speeds. At higher flow speeds and rotational speeds, higher blade loads result in more composite blade deformation (as verified by the structural bending tests), leading to a more significant difference between the composite and aluminum blade shapes.

Similar thrust load trends were observed at both facilities, with approximately 3% lower thrust loads measured for the turbine in the flume. This difference in loads between facilities could be attributed to differences in turbulence intensity; however, a 3% difference is within the uncertainty of the thrust measurements, particularly for the flume tests, which had slightly higher uncertainty.

Figure 7 shows the thrust coefficients at both test facilities for various flow speeds, with separate plots for the composite and aluminum blades. The nondimensional thrust coefficients for the composite BT blades decreased with increasing flow speeds at both facilities. This was particularly evident for the 1.2 m/s test in the flume (triangles in Figure 7), which had a thrust coefficient that was 9% lower than at 0.8 m/s. Higher flow speeds resulted in greater hydrodynamic forces on the BT blades, leading to an increase in passive twisting toward feather. This passive feathering reduces the thrust loads, resulting in reductions in the thrust coefficients, which are more significant at higher flow speeds.

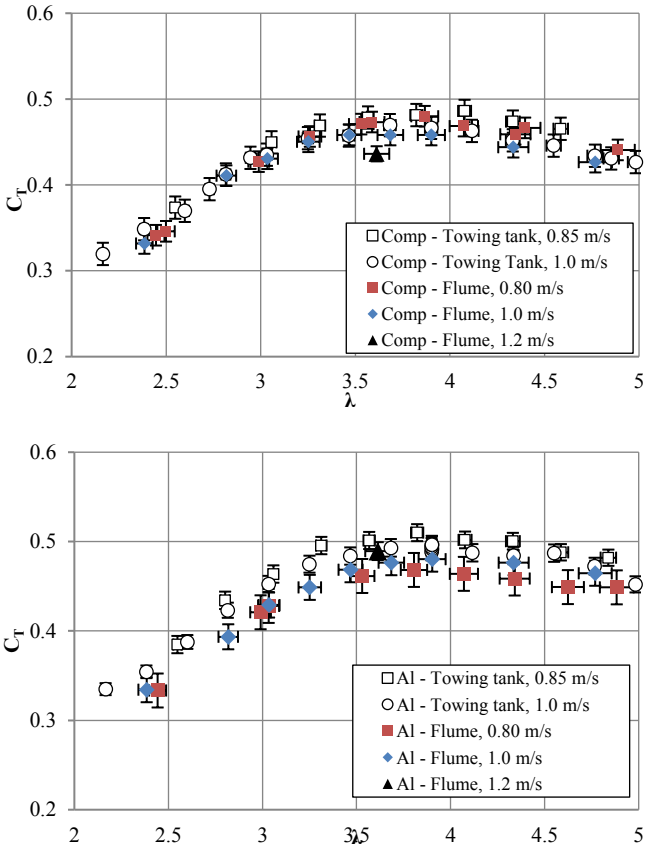

Figure 7 Thrust coefficients: (top) BT composite blades and (bottom) aluminum blades. Flow and rotational speeds varied.

Although the thrust coefficients decreased with increasing flow speeds for the composite BT blades, at 1.2 m/s and $\lambda = 3.6$, the actual thrust on the rotor was 169 N. At 0.8 m/s the thrust was only 83N, as shown in Figure 6. This indicates the

importance of considering the dimensional loading on a tidal turbine, not just the nondimensional load characteristics.

The thrust coefficients for the aluminum blades had less dependence on the flow speed at both facilities. For the tests done in the towing tank, the thrust coefficients for the turbine with aluminum blades decreased slightly with increased flow speed; the flume tests showed the opposite trend, with the 1.2 m/s test having the highest thrust coefficient measured in the tests. At both facilities, however, the differences in the thrust coefficients at the various flow speeds for the aluminum blades were within the margins of error for the thrust measurements. This suggests that the tests could be Reynolds number independent, which is discussed more with respect to the power coefficients in Section III-C.

C. Rotor power

Figure 8 shows the rotor power as a function of rotational speed for the turbine with both composite and aluminum blades at both test facilities. The power was calculated by multiplying the torque measured experimentally by the rotational speed of the rotor.

The power measured for the turbine with composite BT blades was lower at both test facilities, with an 8% reduction in peak power measured in the flume and a 10% reduction in peak power measured in the towing tank. As the rotational speed of the rotor increased, the power was significantly reduced, with a 34% reduction in power at 110 rpm for the composite blades tested in the flume. This would be a useful feature of blades designed for overspeed power regulation [23] and demonstrates the potential for power regulation at high flow speeds. It indicates, however, a decrease in the overall turbine power capture between cut-in and design speeds, which is not desired.

The results of these tests are specific to this particular BT blade design. To limit this unwanted power reduction in future blade designs, investigations using an FSI design tool have indicated that by pretwisting the unloaded blade geometry toward stall, it is possible to achieve load reductions above design conditions while increasing turbine power capture between cut-in and design speeds [10]. Future BT blade designs will be optimized using this concept to limit the reduction in peak power shown in Figure 8.

Figure 9 shows the power coefficients for the turbine with composite BT blades at both facilities under various flow speeds. The BT composite blades generally had lower power coefficients than the aluminum blades, as expected. From Figure 9, the power coefficients for the BT composite blades converged to within 2% at both facilities for the range of flow speeds tested. Because the rigid aluminum blades showed slightly increased power coefficients at high flow speeds, this convergence of power coefficients for the composite blades is attributed to the BT blades twisting, leading to decreased power with increased flow speeds.

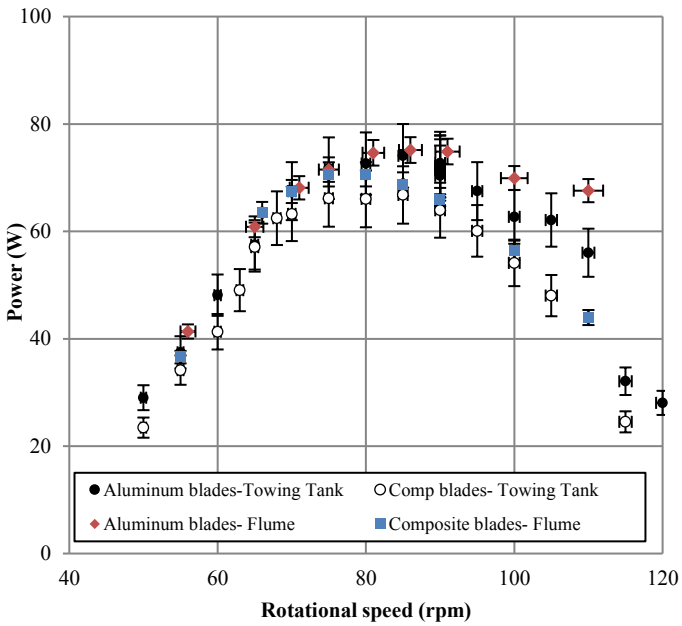

Figure 8 Rotor power for composite BT blades and rigid aluminum blades. Flow speed was1.0 m/s and rotational speeds varied.

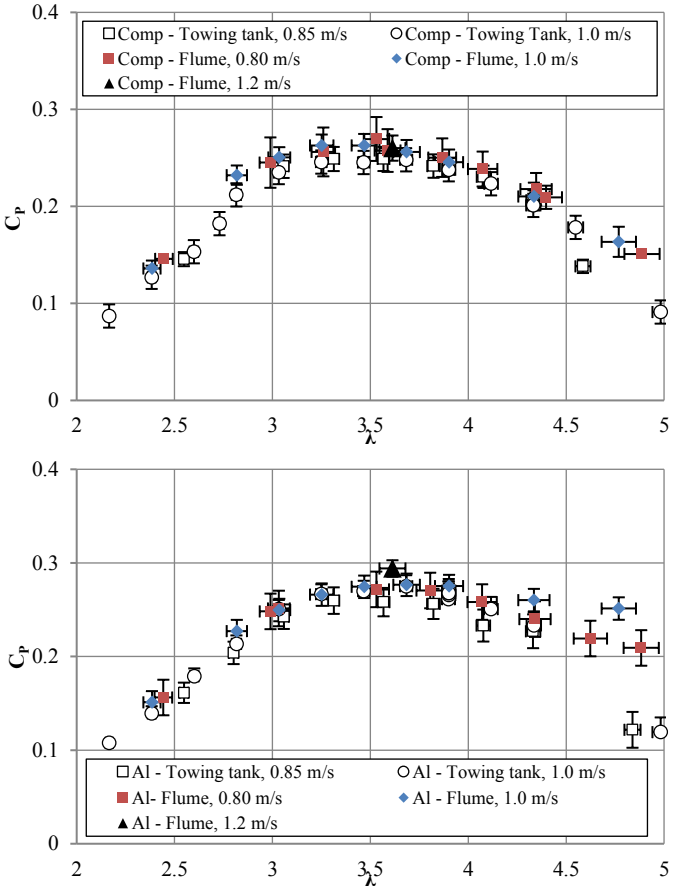

Figure 9 Power coefficients: (top) BT composite blades and (bottom) aluminum blades with varying flow and rotational speeds.

The turbine with aluminum blades had slightly increased power coefficients at higher flow speeds. For example, there was a 6% increase in the power coefficient from 0.8 m/s to 1.2

m/s in the flume, and a 4% increase in the power coefficients between 0.85 m/s and 1.0 m/s in the towing tank.

The chord-Reynolds numbers for these tests ranged from 8 × 10^4 to 2 × 10^5. Previous towing tank tests on a turbine with similar NREL S814 airfoil-shaped blades [24] showed that Reynolds number independence was not reached at chord-Reynolds numbers as high as 1.7 × 10^5. Previous work by Mason-Jones et al. [25] showed that Reynolds number independence was reached at a minimum Reynolds number of 5 × 10^5 for a turbine with Wortmann FX 63-137 airfoil profile blades. These blades differ from the NREL S814 airfoil blades tested in this work. For example, the Wortmann FX 63-137 airfoil has a maximum thickness of 13.7%; the NREL S814 airfoil has a maximum thickness of 24%. As a result, these blades may not perform comparably at low Reynolds numbers. Considering the error bars in the thrust coefficient and power coefficient plots (Figure 7 and Figure 9), it is thought that these tests were Reynolds number independent.

Gaurier et al. [26] performed round robin tests on a 0.70-m-diameter turbine with NACA 63-418 blades at four test facilities (two towing tanks and two circulating tanks). These tests showed that the average power and thrust were similar between facilities, even with turbulence intensities of 3% and blockage ratios ranging from 1.2% to 4.8%. At the two test facilities presented here, the thrust loads measured over the range of test conditions were similar, and the power measured at rotational speeds less than 110 rpm were similar, in agreement with Gaurier et al. For rotational speeds greater than 110 rpm, though, there was significant scatter in the power measured at the two facilities. This is thought to be caused by wear and tear of the seal used in the towing tank tests. The torque-rpm (TGC) calibration used for the towing tank tests was performed several years earlier than these tests using a seal that had been previously used. After the towing tank tests, the seal was removed and found to be worn. The seal was replaced before the flume testing, and the motor TGC was recalibrated with the new seal. The calibration curves were similar for both sets of tests at rotational speeds between 50 and 100 rpm, but diverged at rotational speeds greater than 110 rpm. This suggests that as the seal became worn leading up to the towing tank tests, the TGC calibration at high rotational speeds may have been less accurate than when it was first calibrated. It is also possible that the NREL S814 blades tested in this work could be slightly more sensitive to differences in test conditions such as turbulence than the NACA 63-418 blades Gaurier et al. tested [26].

D. Spectral analysis

The tests presented in this paper were performed under fixed mean flow conditions; however, transient variations in the loads were observed. A spectral analysis using a fast Fourier transform (FFT) was performed on the thrust (in units of [N]) for each test. Figure 10 shows an example of a frequency domain plot for both the composite and aluminum blades for one test case (rotational speed of 80 rpm and flow speed of 1.0 m/s) in the towing tank. Figure 11 shows results for the same test conducted in the flume.

Thrust was measured with a strain gauge on the turbine stanchion. Therefore, an FFT analysis of the thrust loads depicts the fluctuations on the turbine stanchion caused by the hydrodynamic forces acting on the blades, as well as those acting directly on the stanchion.

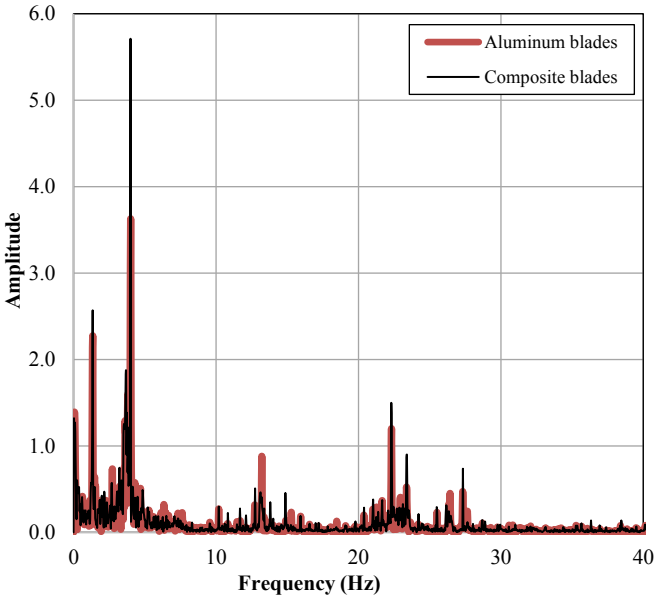

Figure 10 Towing tank tests: thrust signal for the composite and aluminum blades in the frequency domain for a rotational speed of 80 rpm and flow speed of 1.0 m/s (λ = 3.53).

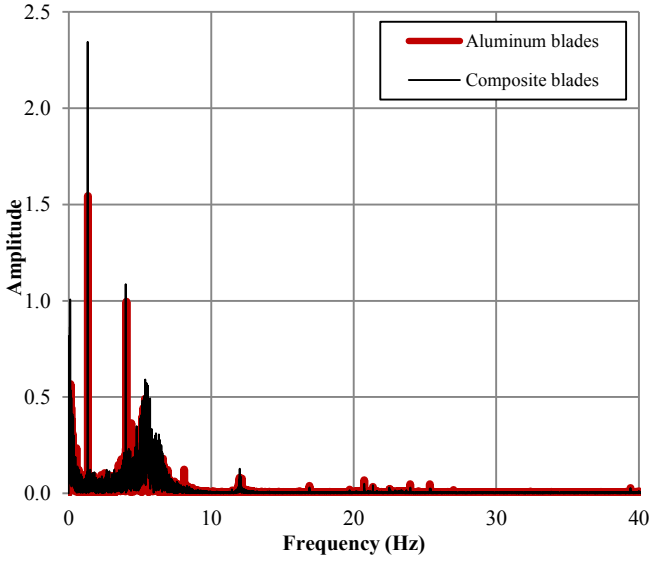

Figure 11 Flume tests: thrust signal for the composite and aluminum blades in the frequency domain for a rotational speed of 80 rpm and flow speed of 1.0 m/s (λ = 3.53).

The turbine with composite and aluminum blades showed comparable dominant frequencies at both test facilities. The FFT results showed that the primary sources of turbine thrust variations were gravitational (occurring at the rotational frequency of the turbine, 1.33 Hz) and blades passing the stanchion (occurring 3 times per revolution, 4 Hz). The natural frequency of the turbine stanchion and frame was also observed in the FFT analysis at both facilities.

An impact test was performed on the stanchion while it was mounted on the towing tank carriage to measure the vibratory response at rest. The higher frequency peaks in Figure 10, occurring around 13 Hz and 22 Hz, coincide with the natural frequency of the stanchion system. Although an impact test was not done on the stanchion while it was mounted in the flume, the peak occurring around 5.4 Hz in Figure 11 is also expected to coincide with the natural frequency of the stanchion, given the different mounting arrangement in the flume.

As illustrated in both Figure 10 and Figure 11, the amplitude of the thrust fluctuations was higher for the turbine with composite BT blades than for the turbine with rigid aluminum blades. The fluctuations were approximately 4.5% and 5.2% of the mean value for the aluminum and composite blades, respectively, in the towing tank, and 3.2% and 4.2% of the mean loads for the aluminum and composite blades, respectively, in the flume. This suggests that dynamic effects from gravity and from the blades passing the stanchion resulted in slightly higher stanchion vibratory loads with the more flexible BT blades in both test facilities. Compared to thrust load variations resulting from turbulence or waves, which have been reported to be as high as 25% [27] and 37% [28], this 5.2% variation in thrust loads is minor. Unsteady loads, however, are an important consideration in the design of HATTs. For this reason, further effects of unsteady loading on the BT blades will be investigated through wave-current testing at IFREMER.

The round robin test results in [26] showed that the highest standard deviation in the loads occurred for the flume facilities and the lowest for the towing tanks. Gaurier et al. concluded that the fluctuating loads were mainly driven by the flow turbulence. For the tests presented here, the flume turbulence intensity was relatively low (1.46% compared to the 3% tested by Gaurier et al. [26]). Therefore, the 1% difference in the load fluctuations measured at the two facilities is more likely attributed to the measurement uncertainty for the thrust and torque, or to slight differences in the rigidity of the stanchion mounting frame and instrumentation.

IV. Conclusions and Future work

In this work, towing tank and flume testing demonstrated that an 828-mm-diameter turbine with composite BT blades had reduced thrust loads compared to the same turbine with geometrically equivalent rigid aluminum blades. Tests showed that the turbine with BT blades had up to 11% lower thrust loads than the turbine with aluminum blades when comparing the mean load for each test. The peak power was also reduced by up to 15%, with the greatest thrust and power reductions occurring at the fastest flow velocities (i.e., higher loads were associated with more extreme conditions). This demonstrates that tailoring the composite layup of HATT blades can potentially reduce the loads, which can lead to overall turbine cost reductions.

The comparison between flexible composite blades and rigid aluminum blades also illustrates the importance of considering FSI in the turbine design process. In this case, modeling the turbine with BT blades without considering the blade deformation (e.g., using stand-alone blade element momentum theory or computational fluid dynamics) would result in a significant overestimate in the rotor loads. This has implications on the design and sizing of other turbine components.

A comparison between the flume and towing tank test facilities showed a good agreement in the average thrust and torque measurements for most test conditions for both blade sets. This agrees with the results presented in Gaurier et al. [26], even with the differences in turbine geometry, blade airfoil shape, and blade flexibility. This confirms, as expected, that tests performed at different facilities with the same flow and rotational speeds should have similar mean thrust and power.

The BT blades tested in this work were designed with the objective of maximizing the thrust load reductions while maintaining structural integrity based on a maximum allowable composite stress. Because of the cost and risk associated with damaging the blades during testing, a high safety factor was used for this blade design. This meant that the blades were stiffer than necessary to withstand the imposed loads during hydrodynamic testing. After building confidence in an FSI design tool by using these test results for verification, future blade designs will have lower, more reasonable safety factors, enabling greater flexibility and a greater reduction in loads. A pretwisted blade shape will also be considered in future designs to increase the turbine power production while still reducing loads and regulating power capture during extreme conditions.

Acknowledgments

The authors thank Tim O'Doherty, Matt Allmark, Carwin Frost, Allan Mason-Jones, and the Cardiff University team for lending the research team their turbine and assisting in towing tank and flume testing. Thank you to the team members at IFREMER for their support during the flume testing period, and to Sandy Day, Charles Keay, Edd Nixon, Grant Dunning, and the team at the Kelvin Hydrodynamics facility for their support during towing tank testing. Thank you to Katie Gracie-Orr and Thomas Nevalainen for the use of their codes. Thank you also to Airborne Marine (Netherlands) for blade manufacturing.

This work was performed using funding from the Natural Sciences and Engineering Research Council of Canada, Killam Trust, the Offshore Energy Research Association of Nova Scotia, the United Kingdom Science and Innovation, and Scottish Development International. Writing of the paper was supported by the U.S. Department of Energy under Contract No. DE-AC36-08GO28308 with the National Renewable Energy Laboratory. Funding was provided by the DOE Office of Energy Efficiency and Renewable Energy, Water Power Technologies Office.

References

1. Neary, V.S., et al., *Methodology for Design and Economic Analysis of Marine Energy Conversion (MEC) Technologies*, in *Sandia Report SAND2014-9040*. 2014.

2. Evans, G. *Maintaining marine turbines*. [Online] 2013; Available from: http://www.power-technology.com/features/feature-maintaining-marine-turbines-tidal-energy/.
3. Mohan, M. *The advantages of composite material in marine renewable energy structures*, in *RINA Marine Renewable Energy Conference*. 2008.
4. King, J. and T. Tryfonas. *Tidal Stream Power Technology – State of the Art*, in *Proc. Oceans*. 2009. Bremen.
5. Grogan, D.M., S.B. Leen, C.R. Kennedy, and C.M. Ó Brádaigh, *Design of composite tidal turbine blades.* Renewable Energy, 2013. **57**: p. 151-162.
6. Motley, M.R. and R.B. Barber, *Passive control of marine hydrokinetic turbine blades.* Composite Structures, 2014. **110**: p. 133-139.
7. Nicholls-Lee, R.F., S.R. Turnock, and S.W. Boyd, *Application of bend-twist coupled blades for horizontal axis tidal turbines.* Renewable Energy, 2013. **50**: p. 541-550.
8. Barber, R.B. and M.R. Motley. *A Numerical Study of the Effect of Passive Control on Cavitation for Marine Hydrokinetic Turbines,* in *EWTEC*. 2015. Nantes, France.
9. Murray, R.E., D.A. Doman, and M.J. Pegg, *Finite Element Modeling and Effects of Material Uncertainties in a Composite Laminate with Bend-Twist Coupling.* Composite Structures, 2015. **121**: p. 362-376.
10. Murray, R.E., T. Nevalainen, K. Gracie-Orr, D.A. Doman, M.J. Pegg, and C.M. Johnstone, *Passively adaptive tidal turbine blades: Design tool development and initial verification.* International Journal of Marine Energy, 2016. **14**: p. 101–124.
11. The European Marine Energy Centre Ltd. *Technology Readiness Levels*. 2014; Available from: http://www.emec.org.uk/services/pathway-to-emec/technology-readiness-levels/.
12. Clarke, J.A., et al., *EquiMar Deliverable 3.2 Concept Appraisal and Tank Testing Practices for 1st Stage Prototype Devices*, in *Equitable Testing and Evaluation of Marine Energy Extraction Devices in Terms of Performance, Cost and Environmental Impact,* 2009.
13. Murray, R.E., *Passively adaptive tidal turbine blades: Design methodology and experimental testing*, PhD Thesis in *Mechanical Engineering*. 2016, Dalhousie University.
14. Doman, D.A., R.E. Murray, M.J. Pegg, K. Gracie-Orr, C.M. Johnstone, and T. Nevalainen, *Tow-tank testing of a 1/20th scale horizontal axis tidal turbine with uncertainty analysis.* International Journal of Marine Energy, 2015. **11**: p. 105-119.
15. Allmark, M., 2016. PhD Thesis, Cardiff University.
16. Ordonez-Sanchez, S., K. Porter, C. Frost, M. Allmark, C. Johnstone, and T. O'Doherty. *Effects of Wave-Current Interactions on the Performance of Tidal Stream Turbines*, in *Asian Wave and Tidal Energy Conference,* 2016.
17. Sicomin, *Sicomin foaming epoxy: PB 170, PB 250, PB 400, PB 600 Cellular epoxy foam production system*. 2009.
18. Karaolis, N., P. Mussgrove, and G. Jeronimidis. *Active and Passive Aeroelastic Power Control Using Asymmetric Fibre Reinforced Laminates for Wind Turbine Blades*. in *10th British Wind Energy Conference*. 1988. London, U.K.
19. Edwin Kanters, A.M., *Personal communication- Blade manufacturing images*. 2015.
20. Zoltek, *Panex 35 Uni-Directional Fabrics*.
21. McCombes, T., C. Johnstone, B. Holmes, L.E. Myers, A.S. Bahaj, and J.P. Kofoed, *EquiMar Deliverable 3.4 Best practice for tank testing of small marine energy devices*, in *Equitable Testing and Evaluation of Marine Energy Extraction Devices in Terms of Performance, Cost and Environmental Impact,* 2010.
22. International Towing Tank Conference, *Recommended Procedures and Guidelines: Guide to the Expression of Uncertainty in Experimental Hydrodynamics*. 2008.
23. Gracie, K., T.M. Nevalainen, C.M. Johnstone, R.E. Murray, D.A. Doman, and M.J. Pegg. *Development of a blade design methodology for overspeed power-regulated tidal turbines*, in *EWTEC*. 2015. Nantes, France.
24. Doman, D.A., R.E. Murray, M.J. Pegg, K. Gracie, C.M. Johnstone, and T. Nevalainen. *Dynamic testing of a 1/20th scale tidal turbine,* in *Asian Wave and Tidal Energy Conference*. 2014. Tokyo, Japan.
25. Mason-Jones, A., et al., *Non-dimensional scaling of tidal stream turbines.* Energy, 2012. **44**(1): p. 820-829.
26. Gaurier, B., et al., *Tidal energy "Round Robin" test comparisons between towing tank and circulating tank results.* International Journal of Marine Energy, 2015. **12**: p. 87-109.
27. Milne, I.A., A.H. Day, R.N. Sharma, and R.G.J. Flay, *Blade loads on tidal turbines in planar oscillatory flow.* Ocean Engineering, 2013. **60**: p. 163-174.
28. Galloway, P.W., L.E. Myers, and A.S. Bahaj. *Studies of a scale tidal turbine in close proximity to waves,* in *3rd International Conference on Ocean Energy*. 2010. Bilbao, Spain.